frontiers in Physics

ORIGINAL RESEARCH
published: 20 May 2021
doi: 10.3389/fphy.2021.691027

Tunable Magnetic Fano Resonances on Au Nanosphere Dimer–Dielectric–Gold Film Sandwiched Structure

*Tianxun Gong, Fang Guan, Zhenjiang Wei, Wen Huang and Xiaosheng Zhang**

State Key Laboratory of Electronic Thin Films and Integrated Devices, School of Electronic Science and Engineering (National Exemplary School of Microelectronics), University of Electronic Science and Technology of China, Chengdu, China

The Fano resonance demonstrates excellent performance due to its narrow asymmetrical spectral line shape, and its sensitivity to structure and material parameter changes. Compared to conventional Fano resonances, the Fano resonance generated by the magnetic dipole is more advantageous because of its high absorption and low loss. In this study, we propose an Au nanosphere dimer–dielectric–gold film sandwiched structure that supports the magnetic Fano resonance mode. And the Fano resonance can be efficiently tuned from visible to near-infrared wavelength by changing the size of the gold nanospheres and the thickness of the dielectric layer. Different from the single gold nanosphere–dielectric–film structure, the results suggest that the proposed structure is sensitive to the polarization direction of the excitation light. Considering the above characteristics, the proposed structure can be applied in multi-band sensing, surface-enhanced Raman spectroscopy, and dynamically adjustable optical switches.

Keywords: Fano resonance, magnetic mode, surface plasmons, Au nanosphere dimer-dielectric-gold film, radiation loss

OPEN ACCESS

Edited by:
Song Sun, China Academy of Engineering Physics, China

Reviewed by:
Kien Voon Kong, National Taiwan University, Taiwan
Taiping Zhang, China Academy of Engineering Physics, China

****Correspondence:***
Xiaosheng Zhang
zhangxs@uestc.edu.cn

Specialty section:
This article was submitted to Optics and Photonics, a section of the journal Frontiers in Physics

Received: *05 April 2021*
Accepted: *13 April 2021*
Published: *20 May 2021*

Citation:
Gong T, Guan F, Wei Z, Huang W and Zhang X (2021) Tunable Magnetic Fano Resonances on Au Nanosphere Dimer–Dielectric–Gold Film Sandwiched Structure. Front. Phys. 9:691027. doi: 10.3389/fphy.2021.691027

INTRODUCTION

Surface plasmon is generated by collective oscillations of photons and electrons [1, 2]. Due to the large radiation loss in the visible light band, surface plasmon resonance has a wide Lorentzian profile resonance peak, which limits its performance [3]. In contrast, Fano resonance originated from the constructive and destructive interference of light and dark modes can effectively suppress the radiation loss and generate strong surface electromagnetic enhancement [4–8]. Furthermore, Fano resonance is drawing intense interest due to its high sensitivity to geometric parameters and the refractive index changes [7, 9–13]. Therefore, Fano resonance can be used in many applications, such as surface-enhanced Raman spectroscopy, surface-enhanced fluorescence, surface plasmon photon chips, resonators, nano-antennas, couplers, biosensors, and optical filtering [14–23].

Most of the researchers who studied Fano resonance focused on the electric effect reflected in the coupling between the electric dipole and the higher-order electric mode [8, 18, 24–26]. Only in recent years, Fano resonance generated by the magnetic mode is being studied [27–29]. However, the mechanisms of magnetic dipole mode have been discussed in previous studies [30, 31]. The magnetic modes can be excited by the sandwiched structure connecting metal layers with a dielectric layer, which is equivalent to a capacitor model. While the two layers of the metal function as two electrodes, opposite charge distributions are generated on the two layers so that a circular displacement current is formed between the metal layers. In such a case, the dipole moment is reduced, which effectively inhibits the loss of the system. According to the present research, organic molecules and two-dimensional materials such as PEG, graphene, and MgF_2, function as dielectric layers [14, 32, 33]. However, the mechanism of effective tuning of the magnetic Fano resonance mode is not studied in depth. In this study, we propose a sandwiched structure composed of an Au dimer and an Au film linked by a dielectric molecule layer, which supports magnetic Fano resonance that can be tuned by the radius of the nanosphere and the thickness of the dielectric layer. Moreover, the proposed structure is sensitive to the polarization direction of the excitation light. Owing to its huge field enhancement brought about by the generation of magnetic mode, the proposed structure has potential applications in improving the sensitivity of multi-band sensing, surface-enhanced Raman spectroscopy, and dynamically adjustable optical switches.

STRUCTURE AND SIMULATION METHOD

The structure was calculated by the finite element method (FEM). A three-dimensional model was developed for the calculation, in which the top and bottom boundaries were set as input port and output port, respectively. For the input port, a normal incident excitation wave with electric field components along the x and/or y direction was adopted during the study. A schematic illustration of the structure is shown in **Figure 1**. As shown in **Figure 1A**, R_1 and R_2 are the radii of two Au nanospheres, respectively. The distance between the two Au nanospheres is fixed at 5 nm. The Au film thickness (D) was fixed at 200 nm. The refractive index of the dielectric layer is 1.469. The thickness of the dielectric layer between the Au nanospheres (radii R_1 and R_2) and the gold film are t_1 and t_2, respectively. The calculated absorption cross-section of the structure with R_1 and R_2 set at 100 nm and t_1 and t_2 set at 1 nm is shown in **Figure 1B**, in which the Fano resonance can be observed with two distinct peaks located at 700 nm (marked as "1") and 900 nm (marked as "2").

RESULTS AND DISCUSSION

The Mechanism of Fano Resonance

To study the mechanism of Fano resonance for the structure, the distribution of the electric field, the magnetic field, and the surface charge corresponding to the structures with R_1 varying from 80 to 120 nm at the two absorption peaks marked as Peak 1 (near 700 nm) and Peak 2 (near 900 nm) are calculated, as shown in **Figures 2C–L**, respectively. The displacement current vector is indicated by the arrow with white color in the distribution of the electric field. As $R_1 = R_2 = 100$ nm and $t_1 = t_2 = 1$ nm, the distribution of the electric field, the magnetic field, and the surface charge at Peak 1 are shown in **Figures 2E**-i, ii, iii, respectively. Two electric current loops formed by the displacement current vector between Au nanospheres with Au film can be observed in the electric field distribution (**Figure 2E**-i). The current loops induce the magnetic mode, which can be seen from the anti-symmetric charge distribution (**Figure 2E**-iii) of the Au nanosphere and the Au film [31]. On the other hand, the electric dipole mode is excited between two spheres, as the magnetic field hotspot between the two spheres is relatively weak (**Figure 2E**-ii). Therefore, the optical properties at Peak 1 are dominated by the magnetic dipole mode. For Peak 2, no current loop could be observed between the Au nanospheres and the gold film (**Figure 2J**-i), while the near-field electric intensity between the nanospheres is relatively strong. Meanwhile, from its surface charge distribution (**Figure 2J**-iii), it can be seen that the electric dipole is located between the two nanospheres. Hence, the optical properties at Peak 2 are

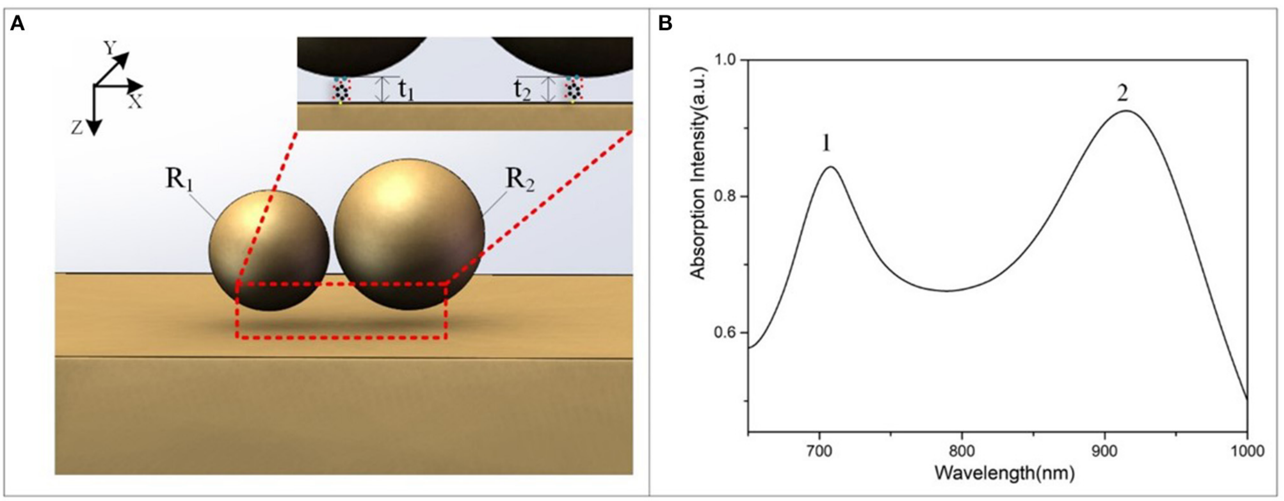

FIGURE 1 | (A) The schematic of Au nanosphere dimer–dielectric–Au film plasmonic nanostructures. The radii of two Au nanospheres are R_1 and R_2, respectively. The thickness of the dielectric layer under two Au nanospheres is t_1 and t_2, respectively. The Au film has a thickness of D. **(B)** The calculated absorption cross-section of the structure ($R_1 = R_2 = 100$ nm, $t_1 = t_2 = 1$ nm, $D = 200$ nm).

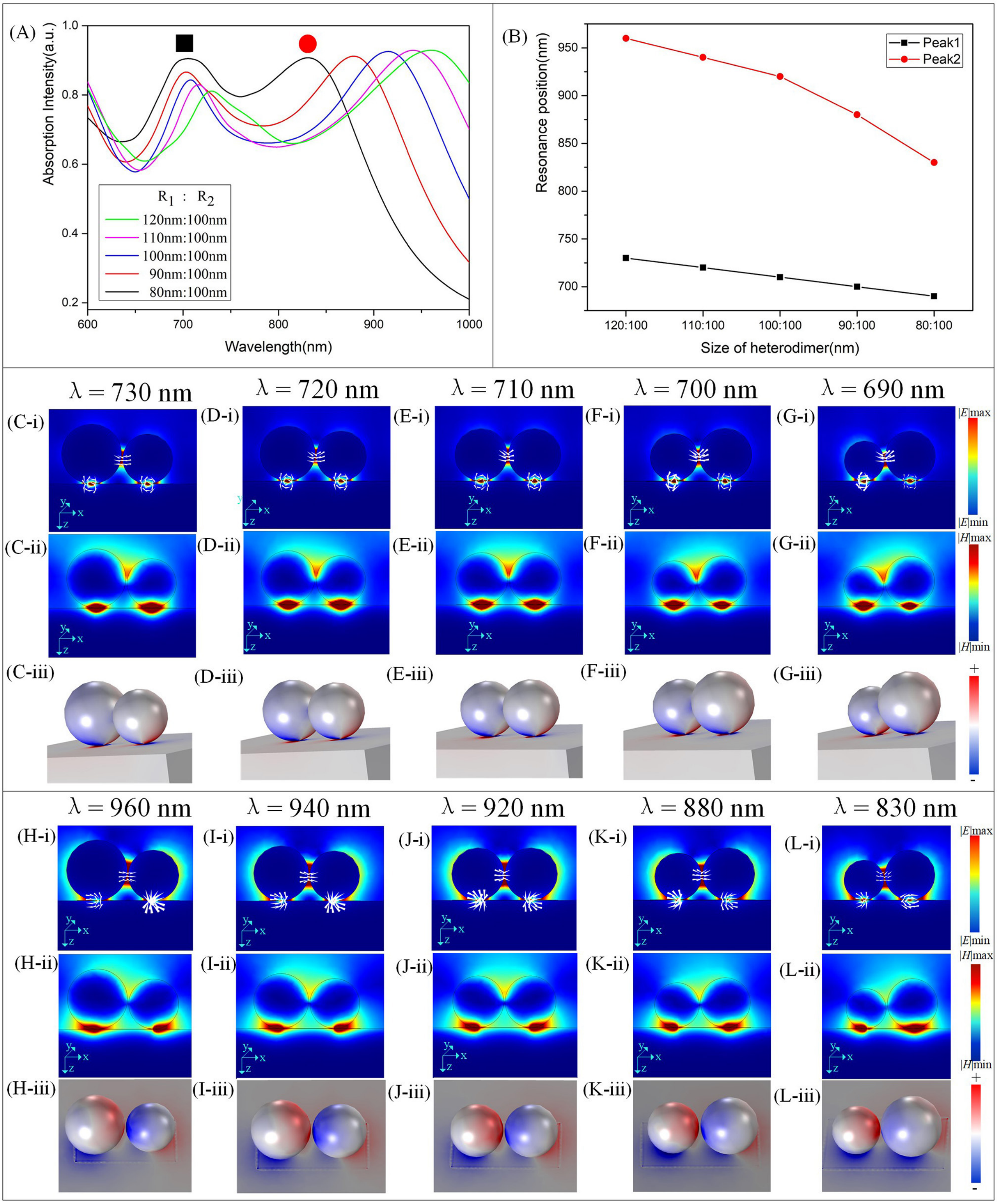

FIGURE 2 | (A) Absorption spectra of Au nanosphere dimer–dielectric–Au film nanostructures with R_1 varied from 120 to 80 nm, while R_2 is fixed at 100 nm. Peak 1 (black square) and Peak 2 (red circle) are marked in the absorption spectrum. **(B)** The resonance peaks as a function of the nanosphere dimer size. **(C–G)** Distribution of the electric field (i), the magnetic field (ii), and the surface charge (iii) at Peak 1 corresponding to the nanosphere dimer with R_1 from 120 to 80 nm. **(H–L)** Distribution of the electric field (i), the magnetic field (ii), and the surface charge (iii) at Peak 2 corresponding to the nanosphere dimer with R_1 from 120 to 80 nm.

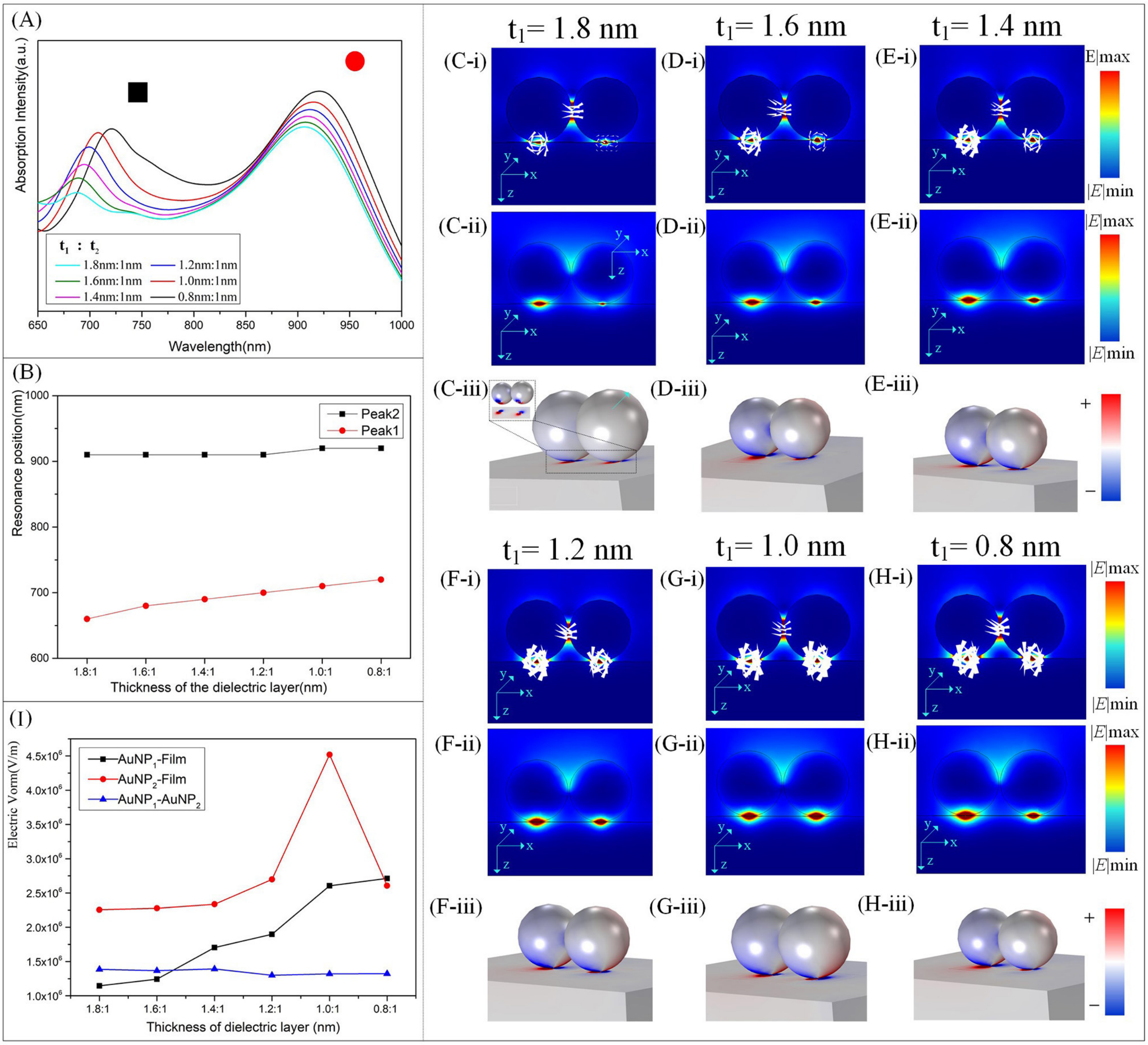

FIGURE 3 | (A) Absorption spectra of the Au nanosphere dimer–dielectric–Au film nanostructures with t_1 varied from 1.8 to 0.8 nm, whereas t_2 is fixed at 1 nm. **(B)** The resonance peaks as a function of the thickness of the dielectric layer. **(C–H)** Distribution of the electric field (i), the magnetic field (ii), and the surface charge (iii) at Peak 1 corresponding to nanosphere dimer with t_1 from 1.8 to 0.8 nm. **(I)** Electric field enhancement of three hot spots at Peak 1 as a function of t_1.

dominated by the electric dipole mode, and the hotspot between Au nanospheres and Au film in the magnetic field distribution (**Figure 2J**-ii) is not extremely localized compared with that of Peak 1 (**Figure 2E**-ii). Therefore, the generation of the Fano resonance is due to the coupling of the two modes: the magnetic dipole mode as the dark mode with the smaller net dipole moment and the electric dipole mode as the bright mode.

Effects of Nanosphere Radius

The effects of the R_1 on Fano resonance are also studied. **Figure 2A** shows the absorption spectrum of the structure with R_1 tuning from 80 to 120 nm. As R_1 increases, in addition to a redshift of both peaks 1 and 2, a slight broadening of the Fano dip is also observed in the spectrum. As shown in **Figure 2B**, the location of Peak 1 shifted from 690 to 730 nm, and Peak 2 shifted from 830 to 960 nm. Despite the changes in R_1, the magnetic dipole mode between the Au nanosphere dimer and the Au film dominates at Peak 1. There is an obvious current loop observed in the electric field distribution (**Figures 2C–G**-i), and the surface charge distribution is anti-phase symmetrical (**Figures 2C–G**-iii). The electric dipole mode dominates at Peak 2, which can be observed from **Figures 2H–L**. In the meantime, as the R_1 radius increases, the magnetic field intensity and electric dipole forces also increase, resulting in the enhancement of the near-field interaction in the system. As a result, the mode shifts to lower energies, and the Fano dip is broadened [34].

Effects of the Dielectric Layer Thickness

The influence of t_1 on Fano resonance is also studied. **Figure 3A** shows the absorption spectrum of the structure with t_1 from 0.8 to 1.8 nm. With the decrease in the t_1, the shifts of the two resonance peak positions are shown in **Figure 3B**. There was an insignificant shift in the position of Peak 2, which was fixed around 920 nm. As Peak 2 originated from the mutual coupling between the two Au nanospheres, the variation in the dielectric layer thickness has little effect on the relative positions of the two Au nanoparticles. The change in the coupling degree and the electric dipole moment was insignificant; therefore, the position of Peak 2 was almost unchanged. On the contrary, as t_1 decreased from 1.8 to 0.8 nm, the position of Peak 1 (red) shifted from 660 to 720 nm. **Figures 3C–H** shows the distribution of electric field (i), magnetic field (ii), and surface charge (iii) when the dielectric layer thickness t_1 decreased from 1.8 to 0.8 nm. The magnetic dipole force between the Au nanospheres R_1 and the Au film connected by the dielectric layer with a thickness of t_1 continuously decreased, and the magnetic field hotspots became stronger. In addition, it was found that plasmon mode and intensity excited between the Au nanosphere R_2 and the Au film connected by the dielectric layer with a thickness of t_2 were also affected. When the thickness t_1 was 1.8 nm, the magnetic quadrupole mode was excited between the Au nanosphere R_2 and the Au film, as shown in **Figure 3C**-iii. The inset is the detailed schematic diagram of the charge distribution at the junction. However, due to the low displacement current density, the localized near-field magnetic intensity becomes weak [29]. Apart from the case of 1.8 nm, as t_1 decreases from 1.6 to 0.8 nm, the magnetic dipole mode is stimulated at the junction of the nanosphere with a radius of R_2 and the film (with a thickness of t_1), as shown in **Figures 3D–H**-i. The electric and magnetic intensities reached the highest when t_1 was 1 nm and gradually decreased with an increase in t_1, as shown in **Figure 3I**. It was also observed from the near-field electric intensity at the three

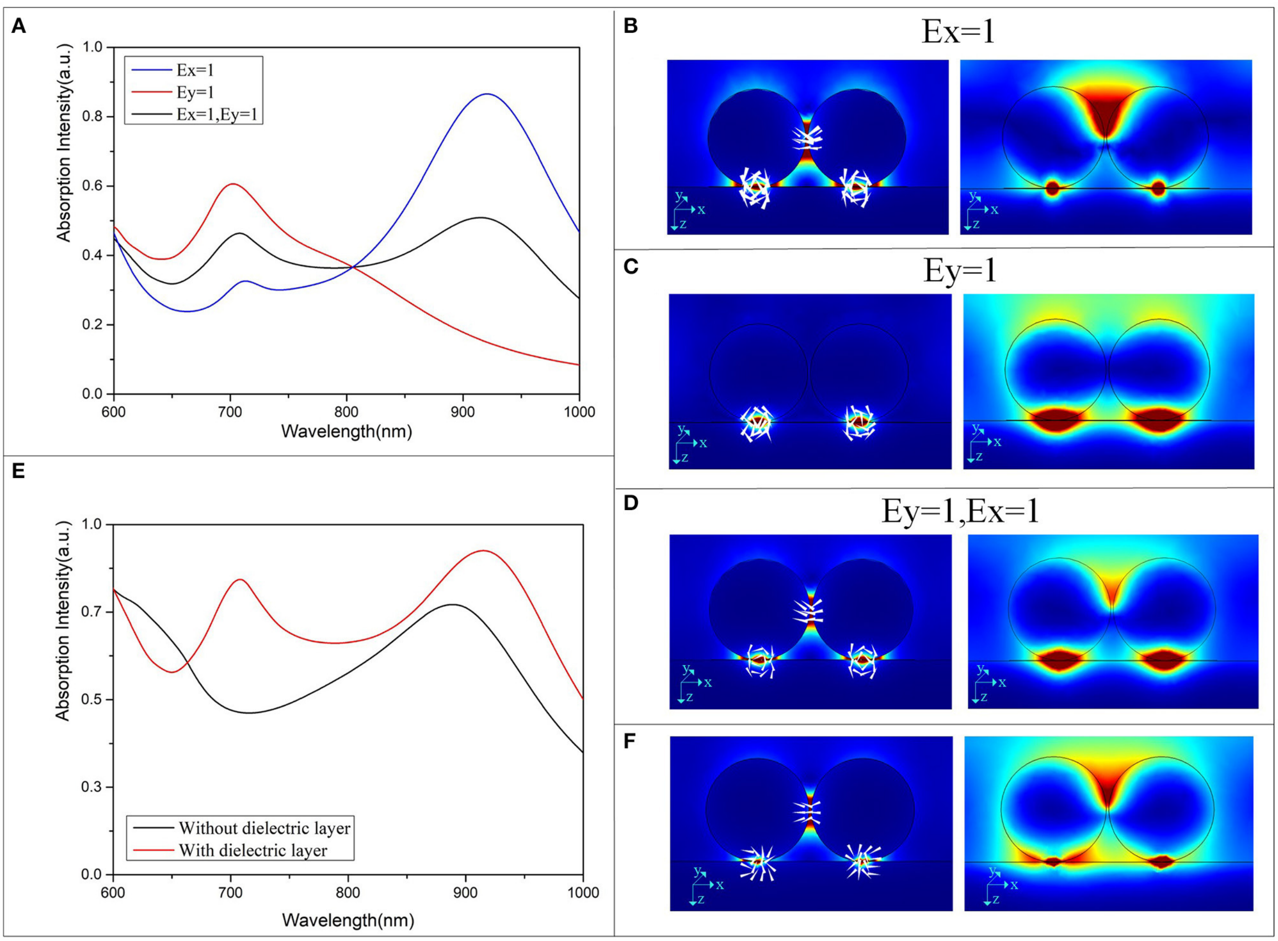

FIGURE 4 | (A) Absorption spectra of Au nanosphere dimer–dielectric–gold film structure with different polarization directions. **(B–D)** Distribution of the electric field (left) and the magnetic field (right) located at 710 nm corresponding to Ex = 1, Ey = 1, and Ex = Ey = 1. **(E)** The absorption spectra of the structure with and without the dielectric layer. **(F)** Distribution of the electric field (left) and the magnetic field (right) located at 710 nm corresponding to the structure without the dielectric layer.

hotspots that are located between the nanosphere with radius R_1 and the nanosphere with radius R_2 ($AuNP_1$-$AuNP_2$), between the nanosphere with radius R_1 and the Au film ($AuNP_1$-Film), and between the nanosphere with radius R_2 and the Au film ($AuNP_2$-Film). There was an insignificant change in the intensity at the hotspot of $AuNP_1$-$AuNP_2$ with a decrease in t_1, and the hotspot of $AuNP_1$-Film decreased, while the hotspot of $AuNP_2$-Film reached maximum when t_1 was 1 nm.

Effects of the Polarization Direction

Considering the mutual coupling between the two nanospheres, the optical properties and the near-field enhancement effect are also studied when the polarization direction of the incident light is changed. **Figure 4A** shows the absorption spectra of the Au nanosphere dimer–dielectric–Au film structure under the incident light with different polarization directions. It can be seen that the polarization direction has little effect on the peak around 700 nm, whereas the peak around 900 nm strongly depends on the electric field polarization in the x direction. In other words, as long as the electric field has a component along the x direction where the two spheres contact, the dipole mode between the two nanospheres can be excited. It is also confirmed that the absorption peak around 900 nm originated from the electric dipole between the two nanospheres. **Figures 4B–D** shows the distribution of the electric field (left) and the magnetic field (right) corresponding to the absorption peak near 700 nm for the incident light with different polarization directions. A clear current loop and localized magnetic hot spots are generated between the Au nanospheres and the Au film around 700 nm, suggesting that the magnetic mode is almost unaffected by the polarization direction of the electric field.

To further investigate the effect of the dielectric layer in exciting the magnetic mode, the absorption spectrum of the structure without the dielectric layer was calculated, as shown in **Figure 4E**. Compared to the structure with the dielectric layer, the absorption peak of the one without dielectric layer at around 700 nm disappeared and its corresponding displacement current loop is non-existent (**Figure 4F**), which further proved the vital role of the dielectric layer to excite the magnetic mode of the structure [24].

CONCLUSIONS

Our study proposes an Au nanosphere dimer–dielectric–gold film sandwiched structure that generates magnetic field-based Fano resonance from visible to near-infrared wavelength. By changing the size of the gold nanosphere and the thickness of the dielectric layer, the Fano resonance wavelength and the resonance intensity can be easily tuned. The proposed structure is also sensitive to the incident polarization direction. Owing to its flexible tuning, high absorption, and low loss characteristics, this structure has a great potential in applications such as resonators, surface-enhanced Raman scattering, and nano-antennas.

DATA AVAILABILITY STATEMENT

The raw data supporting the conclusions of this article will be made available by the authors, without undue reservation.

AUTHOR CONTRIBUTIONS

FG and ZW modeled the problem. TG, FG, and WH explored the solution and carried out numerical computations. FG and XZ analyzed the finding of the study. All authors reviewed the manuscript.

FUNDING

The authors acknowledge the financial support from the National Natural Science Foundation of China (61905035).

REFERENCES

1. Sipova-Jungova H, Jurgova L, Mrkvova K, Lynn NS, Spackova B, Homola J. Biomolecular charges influence the response of surface plasmon resonance biosensors through electronic and ionic mechanisms. *Biosens Bioelectron.* (2019) 126:365–72. doi: 10.1016/j.bios.2018.11.002
2. Zhang X, Liu F, Yan X, Liang L, Wei D. Symmetric and antisymmetric multipole electric-magnetic fano resonances in elliptic disk-nonconcentric split ring plasmonic nanostructures. *J Optics.* (2020) 22. doi: 10.1088/2040-8986/abbf8b
3. Tiguntseva EY, Baranov DG, Pushkarev AP, Munkhbat B, Komissarenko F, Franckevicius M, et al. Tunable hybrid fano resonances in Halide perovskite nanoparticles. *Nano Lett.* (2018) 18:5522–9. doi: 10.1021/acs.nanolett.8b01912
4. Luk'yanchuk B, Zheludev NI, Maier SA, Halas NJ, Nordlander P, Giessen H, et al. The fano resonance in plasmonic nanostructures and metamaterials. *Nat Mater.* (2010) 9:707–15. doi: 10.1038/nmat2810
5. Nazir A, Panaro S, Proietti Zaccaria R, Liberale C, De Angelis F, Toma A. fano coil-type resonance for magnetic hot-spot generation. *Nano Lett.* (2014) 14:3166–71. doi: 10.1021/nl500452p
6. Limonov MF, Rybin MV, Poddubny AN, Kivshar YS. Fano resonances in photonics. *Nat Photonics.* (2017) 11:543–54. doi: 10.1038/nphoton.2017.142
7. Cao G, Dong S, Zhou LM, Zhang Q, Deng Y, Wang C, et al. Fano resonance in artificial photonic molecules. *Adv Optical Mater.* (2020) 8:1902153. doi: 10.1002/adom.201902153
8. Pena-Rodriguez O, Diaz-Nunez P, Gonzalez-Rubio G, Manzaneda-Gonzalez V, Rivera A, Perlado JM, et al. Au@Ag core-shell nanorods support plasmonic fano resonances. *Sci Rep.* (2020) 10:5921. doi: 10.1038/s41598-020-62852-9
9. Lassiter JB, Sobhani H, Fan JA, Kundu J, Capasso F, Nordlander P, et al. fano resonances in plasmonic nanoclusters: geometrical and chemical tunability. *Nano Lett.* (2010) 10:3184–9. doi: 10.1021/nl102108u
10. Ding J, Arigong B, Ren H, Shao J, Zhou M, Lin Y, et al. Dynamically tunable fano metamaterials through the coupling of graphene grating and square closed ring resonator. *Plasmonics.* (2015) 10:1833–9. doi: 10.1007/s11468-015-0003-6
11. Zhou C, Huo Y, Nini C, Jiang X, Guo Y, Hou Y, et al. Generation and manipulation of the fano resonance with high refractive index sensitivity based on the square split ring dimer. *Mater Res Exp.* (2019) 6:105064. doi: 10.1088/2053-1591/ab3b85
12. Bazgir M, Zarrabi FB. A switchable split ring resonator nanoantenna design with organic material composite as a refractive index sensor. *Optics Commun.* (2020) 475:126211. doi: 10.1016/j.optcom.2020.126211

13. Modi KS, Kaur J, Singh SP, Tiwari U, Sinha RK. Extremely high figure of merit in all-dielectric split asymmetric arc metasurface for refractive index sensing. *Optics Commun.* (2020) 462:125327. doi: 10.1016/j.optcom.2020.125327
14. Moreau A, Ciraci C, Mock JJ, Hill RT, Wang Q, Wiley BJ, et al. Controlled-reflectance surfaces with film-coupled colloidal nanoantennas. *Nature.* (2012) 492:86–9. doi: 10.1038/nature11615
15. Ding S-Y, Yi J, Li J-F, Ren B, Wu DY, Panneerselvam R, et al. Nanostructure-based plasmon-enhanced Raman spectroscopy for surface analysis of materials. *Nat Rev Mater.* (2016) 1:1–16. doi: 10.1038/natrevmats.2016.36
16. Kurouski D, Large N, Chiang N, Henry A-I, Seideman T, Schatz GC, et al. Unraveling the near- and far-field relationship of 2d surface-enhanced Raman spectroscopy substrates using wavelength-scan surface-enhanced Raman excitation spectroscopy. *J Phys Chem C.* (2017) 121:14737–44. doi: 10.1021/acs.jpcc.7b04787
17. Qin F, Lai Y, Yang J, Cui X, Ma H, Wang J, et al. Deep fano resonance with strong polarization dependence in gold nanoplate-nanosphere heterodimers. *Nanoscale.* (2017) 9:13222–34. doi: 10.1039/C7NR04524G
18. Ai B, Song C, Bradley L, Zhao Y. Strong fano resonance excited in an array of nanoparticle-in-ring nanostructures for dual plasmonic sensor applications. *J Phys Chem C.* (2018) 122:20935–44. doi: 10.1021/acs.jpcc.8b05154
19. Dutta A, Alam K, Nuutinen T, Hulkko E, Karvinen P, Kuittinen M, et al. Influence of fano resonance on SERS enhancement in Fano-plasmonic oligomers. *Opt Express.* (2019) 27:30031–43. doi: 10.1364/OE.27.030031
20. Li J, Deng TS, Liu X, Dolan JA, Scherer NF, Nealey PF. Hierarchical assembly of plasmonic nanoparticle heterodimer arrays with tunable Sub-5 nm nanogaps. *Nano Lett.* (2019) 19:4314–20. doi: 10.1021/acs.nanolett.9b00792
21. Luo X, Xing Y, Galvan DD, Zheng E, Wu P, Cai C, et al. Plasmonic gold nanohole array for surface-enhanced Raman scattering detection of DNA methylation. *ACS Sens.* (2019) 4:1534–42. doi: 10.1021/acssensors.9b00008
22. Mahmoudpour M, Ezzati Nazhad Dolatabadi J, Torbati M, Homayouni-Rad A. Nanomaterials based surface plasmon resonance signal enhancement for detection of environmental pollutions. *Biosens Bioelectron.* (2019) 127:72–84. doi: 10.1016/j.bios.2018.12.023
23. Chow TH, Lai Y, Lu W, Li N, Wang J. Substrate-Enabled Plasmonic Color Switching with Colloidal Gold Nanorings. *ACS Mater Lett.* (2020) 2:744–53. doi: 10.1021/acsmaterialslett.0c00182
24. Cui X, Qin F, Lai Y, Wang H, Shao L, Chen H, et al. Molecular tunnel junction-controlled high-order charge transfer plasmon and fano resonances. *ACS Nano.* (2018) 12:12541–50. doi: 10.1021/acsnano.8b07066
25. Du K, Li P, Gao K, Wang H, Yang Z, Zhang W, et al. Strong coupling between dark plasmon and anapole modes. *J Phys Chem Lett.* (2019) 10:4699–705. doi: 10.1021/acs.jpclett.9b01844
26. Chen Z, Zhang S, Chen Y, Liu Y, Li P, Wang Z, et al. Double fano resonances in hybrid disk/rod artificial plasmonic molecules based on dipole-quadrupole coupling. *Nanoscale.* (2020) 12:9776–85. doi: 10.1039/D0NR00461H
27. Shafiei F, Monticone F, Le KQ, Liu XX, Hartsfield T, Alu A, et al. A subwavelength plasmonic metamolecule exhibiting magnetic-based optical fano resonance. *Nat Nanotechnol.* (2013) 8:95–9. doi: 10.1038/nnano.2012.249
28. Liu K, Xue X, Sukhotskiy V, Furlani EP. Optical fano resonance in self-assembled magnetic–plasmonic nanostructures. *J Phys Chem C.* (2016) 120:27555–61. doi: 10.1021/acs.jpcc.6b09473
29. Jiang X, Huo Y, Zhou C, Guo Y, Hou Y, Niu Q. High-order magnetic modes and multiple Fano resonances generation by a fish-like dimer nanostructure. *Phys Scrip.* (2020) 95:055507. doi: 10.1088/1402-4896/ab7850
30. Tang C, Yan Z, Wang Q, Chen J, Zhu M, Liu B, et al. Ultrathin amorphous silicon thin-film solar cells by magnetic plasmonic metamaterial absorbers. *RSC Adv.* (2015) 5:81866–74. doi: 10.1039/C5RA15177E
31. Chen S, Zhang Y, Shih TM, Yang W, Hu S, Hu X, et al. Plasmon-induced magnetic resonance enhanced Raman spectroscopy. *Nano Lett.* (2018) 18:2209–16. doi: 10.1021/acs.nanolett.7b04385
32. Ni X, Wong ZJ, Mrejen M, Wang Y, Zhang X. An ultrathin invisibility skin cloak for visible light. *Science.* (2015) 349:1310–4. doi: 10.1126/science.aac9411
33. Liu B, Tang C, Chen J, Zhu M, Pei M, Zhu X. Electrically tunable fano resonance from the coupling between interband transition in monolayer graphene and magnetic dipole in metamaterials. *Sci Rep.* (2017) 7:17117. doi: 10.1038/s41598-017-17394-y
34. Dregely D, Hentschel M, Giessen H. Excitation and tuning of higher-order fano resonances in plasmonic oligomer clusters. *ACS Nano.* (2011) 5:8202–11 doi: 10.1021/nn202876k

Conflict of Interest: The authors declare that the research was conducted in the absence of any commercial or financial relationships that could be construed as a potential conflict of interest.